Aging and solid or liquid behavior in pastes

Philippe Coussot, Xavier Chateau, Laurent Tocquer, Hervé Tabuteau, G. Ovarlez

Aging and solid or liquid behavior in pastes

P. Coussot[a)]

Institut Navier, 2 Allee Kepler Champs sur Marne, France

H. Tabuteau

Department of Physics and Astronomy, University of Western Ontario, London, N6A3K7 Ontario, Canada

X. Chateau, L. Tocquer, and G. Ovarlez

Institut Navier, 2 Allee Kepler Champs sur Marne, France

(Received 14 April 2006; final revision received 11 July 2006)

Synopsis

We carried out systematic creep tests after different times of rest and over sufficiently long times with pasty materials of various internal structures in a Couette geometry. From an analysis of the data taking into account the inertia of the system and the heterogeneous distribution of stress, we show that: (i) for a stress below the yield stress these materials remain solid but undergo residual, irreversible deformations over long time which exhibit some trends typical of aging in glassy systems; (ii) as a result of thixotropy (or aging) in the solid regime the elastic modulus increases logarithmically with the time of rest; (iii) in the liquid regime the effective behavior of the material can be well represented by a truncated power-law model; (iv) a fundamental parameter of the solid-liquid transition is a critical effective shear rate (associated with the yield stress) below which the material cannot flow steadily. © *2006 The Society of Rheology.* [DOI: 10.1122/1.2337259]

I. INTRODUCTION

Many materials of industrial importance such as paints, mining suspensions, printing inks, foodstuffs, drilling fluids, cement pastes, foams, etc., are pasty materials exhibiting an apparent yield stress which may be determined with the help of various techniques and procedures [Coussot (2005)]. The effectiveness of the existence of this yield stress was the subject of some debate [Barnes and Walters (1985)] and, although it was concluded that the yield stress is an engineering reality [Hartnett and Hu (1989); Astarita (1990), Spaans and Williams (1995)], the origin of extremely slow flows for stresses below the apparent yield stress [Barnes (1999)] has not been much discussed yet in literature. Besides, pasty materials also often appear as materials exhibiting thixotropy, generally understood as an increase of the apparent viscosity at rest and a decrease under shear [Mewis (1979); Barnes (1997)]. Although satisfactory models have been proposed for modeling simple yield stress fluids [Bird *et al.* (1982)], this is not the case for modeling

[a)]Author to whom correspondence should be addressed; electronic mail: philippe.coussot@lcpc.fr

thixotropy, for which various models have been suggested [Chan Man Fong *et al.* (1994); Usui (1995); Mujumdar *et al.* (2001); Coussot *et al.* (2002b); Roussel *et al.* (2004); Huynh *et al.* (2005); Dullaert and Mewis (2005)] but not confirmed by a comparison with systematic measurements under very different experimental conditions. This difficulty results from the much more complex characteristics to be taken into account for describing thixotropy. Finally, thixotropy is often not taken into account in practice, because of a lack of simple, systematic, relevant procedures to characterize it. We also remark that, even if some of these mechanical models assumed the existence of a (sometimes time-dependent) yield stress, they generally considered thixotropy as a property independent of yielding. Recently, it was nevertheless suggested that thixotropy and yielding are two intimately linked properties [Coussot *et al.* (2002a)].

Recently, pasty materials, which exhibit both a solid and a liquid regime, also became the object of strong interest from physicists who see in them a specific class of materials, namely soft-jammed systems, capable of undergoing a kind of glass transition at ambient temperature. Thus, the similarity of jammed systems with glassy materials might help clarify some aspects of glass behavior [Bonn *et al.* (1999)]. At this stage two common qualitative characteristics of soft-jammed systems have been identified, namely jamming and aging [Liu and Nagel (1998)], respectively, associated with the existence of a network of interactions between elements in the liquid and with the out-of-equilibrium character of these systems made of a great number of elements undergoing rearrangement due to thermal agitation. These two characteristics are in fact directly related to two basic mechanical properties: yielding and thixotropy, which shows that these physical properties can be studied at a macroscopic scale. Recently, aging characteristics similar to glasses [Struik (1978)] were shown for model colloidal gels [Cloitre *et al.* (2000); Derec *et al.* (2000); Cipelletti *et al.* (2000)] with, for some aspects, straightforward relationships with internal structure [Cloitre *et al.* (2003); Ramos and Cipelletti (2005)]. Besides, there have been recently nice predictions of the elastic [Seth *et al.* (2006)] or viscoelastic [Shah *et al.* (2003)] properties of particulate gels from the particle interactions and significant progress in the understanding of the "cage effects" in dense suspensions [Gopalakrishnan *et al.* (2004)]. At last some original aspects of aging in colloidal systems [Viasnoff and Lequeux (2002)] were explained by a modified version of the soft-glassy-rheology model [Sollich *et al.* (1997); Hébraud and Lequeux (1998)]. The complete predictions in terms of yielding and aging of this promising rheophysical model was reviewed by Fielding *et al.* (2000).

In order to progress in this field, it seems useful to identify general rheophysical properties predicted by some physical theoretical model. However, recent observations have shown that the flow of soft-jammed systems may be more complex than expected from basic yield stress models: flow curve with a minimum indicating some flow instability [Coussot *et al.* (1993); Cheng (2003)]; shear-banding, although homogeneous flow was expected for concentrated suspensions [Mas and Magnin (1994); Pignon *et al.* (1996); Coussot *et al.* (2002c); Varadan and Solomon (2003)]; foams [Rodts *et al.* (2005)]; emulsions [Becu *et al.* (2004)] and micellar solutions [Cappelaere *et al.* (1997); Britton and Callaghan (1997); Decruppe *et al.* (2001); Salmon *et al.* (2003); Hu and Lips (2005)]; viscosity bifurcation around a critical stress [Coussot *et al.* (2002a, b); Da Cruz *et al.* (2002)]; apparent wall slip with rough walls [Herzhaft *et al.* (2003)]. This suggests that one still has to identify the fundamental, generic rheological properties of these materials, as they might not be exactly those retained up to now.

Here, we intend to get a further view of the effective, common characteristics of the mechanical behavior of aging jammed systems. In this aim we chose three soft-jammed systems of very different internal structures, and carried out careful and systematic creep

tests with different stress values and times of rest. We thus could observe more precisely the characteristics of the solid-liquid transition and the characteristics of aging at rest. In particular we show that (i) for a stress below the yield stress these materials remain solid but undergo residual, irreversible deformations over long time which exhibit some trends typical of aging in glassy systems; (ii) as a result of thixotropy (or aging) in the solid regime the elastic modulus increases logarithmically with the time of rest; (iii) in the liquid regime the effective behavior of the material can be well represented by a truncated power-law model, (iv) a fundamental parameter of the solid-liquid transition is a critical effective shear rate (associated with the yield stress) below which the material cannot flow steadily. We start by presenting the materials and procedures (Sec. II). Then, we report the results and analyze them (Sec. III). Finally, we propose some further physical interpretation of these results (Sec. IV).

II. MATERIALS AND PROCEDURES

A. Materials

We used a bentonite suspension at a solid volume fraction of $\phi=5\%$ (see characteristics of material and preparation in [Coussot *et al.* (2002a)]), a mustard (Maille, France), and a hair gel (Vivelle Dop, France). Here, we will simply give basic elements concerning the internal structure of these materials. The bentonite suspension is made of (smectite) clay particles of maximum length of the order of 1 μm and of large aspect ratio (of the order of 100). Water molecules of the suspending phase tend to penetrate between the elementary layers composing each particle, which thus swell. As a consequence, in a given volume of water these colloidal particles are squeezed against each other but also interact via electrostatic forces due to the existence of exchangeable cations forming a double layer at some distance from the particle surface. The structure is finally heterogeneous at a local scale, mainly composed of particle stacks and pure water volumes [see for example Roy *et al.* (2000)], but still forms a continuous network. The mustard is a mixture of water, vinegar, mustard seed particles, mustard oil, and various acids. This is a complex material that we can see as a suspension in an oil-in-water emulsion with a large concentration of elements (droplets and particles). The hair gel is mainly made of Carbopol in water. The structure of a Carbopol suspension is liable to depend on the exact characteristics of the material used, but in general its molecules arrange in roughly spherical blobs, which tend to swell in water [see for example Carnali and Naser (1992)]. As a consequence, beyond a critical concentration the blobs are squeezed against each other. The common characteristics of these three materials is that, due to the large concentration of their elements (particles, droplets, blobs) which "softly" interact when immersed in a liquid, they form a "soft-jammed" structure.

B. Procedures

The reproducibility and relevance of rheometrical data with jammed systems especially for long duration tests is challenging because various perturbating effects can occur such as wall slip, drying, edge effects, phase separation, etc. [Coussot (2005)]. In order to avoid these problems we used a controlled stress Bohlin C-VOR200 rheometer equipped with a Couette geometry (outer cylinder radius: $r_2=18$ mm) with a rough surface (roughness: 0.3 mm) and a six-blade vane (envelope radius: $r_1=12.5$ mm; height: $h=45$ mm) as inner rotating part. This geometry yields a flow very close to that for a simple coaxial cylinder geometry [Barnes and Nguyen (2001); Raynaud *et al.* (2002)] and ensures negligible wall slip. Thus, in the following we will consider this geometry as a Couette one. In order to avoid edge effects the vane bottom was situated at 2 cm from the cup bottom

so that the torque needed to shear the material below the vane was generally much smaller than the torque needed to shear the material comprised in the gap between the vane and the outer cylinder. In particular for incipient flows, when the shear stress is close to the yield stress, the contribution to torque from the material below the vane is about ten times smaller than that from the material in the radial gap. At last the rheometer geometry was surrounded by a wet sheet in order to minimize drying effects. The ambient temperature was maintained at 20 °C for all tests.

After its preparation each material was set up in the geometry and presheared during 60 s at a large apparent shear rate, $\dot{\gamma}_p$, so as to reach a state of "rejuvenation" of reference (mustard: $\dot{\gamma}_p = 200\ s^{-1}$; gel: $\dot{\gamma}_p = 100\ s^{-1}$; bentonite: $\dot{\gamma}_p = 300\ s^{-1}$). Note that the exact conditions of rejuvenation can play a role in the behavior of the material observed afterwards but we did not study that point in detail. Then, the sample was left at rest (stress equal to zero) for a time t_w and a finite shear stress level was applied at $t=0$, which is taken as the origin of time. The origin of deformation is also taken at this time. Suddenly dropping the stress to zero effectively does not stop the flow, but in our tests the rapid decrease of the rotor rotation velocity seemed to take not more than 1 s, so that the structure recovery at rest should not be affected by this residual flow as long as $t_w \gg 1$ s. For each material we carried out systematic creep tests under different torque levels for a given value of t_w, and systematic creep tests after different values of t_w for a given stress level below the yield stress. We also carried out strain relaxation tests by releasing the stress after different times of creep flow t_w' for a given time of rest. Some dynamic tests were carried out with a stress amplitude of 0.1 Pa and a frequency $f_0 = 1$ Hz.

C. Interpretation of measurements

Under usual assumptions (negligible inertia and edge effects) it may be shown [Coleman *et al.* (1966)] that in the gap the *effective shear stress* at the distance r is

$$\tau_{\text{eff}}(r) = \frac{M}{2\pi h r^2}, \tag{1}$$

where M is the torque applied on the inner tool, while in the limit of small deformations the amplitude of the *effective deformation* (γ) in time (t) is

$$\gamma_{\text{eff}}(r) = -r\frac{d\delta}{dr}, \tag{2}$$

in which δ is the local angle of rotation, and the amplitude of the *effective shear rate*, $\dot{\gamma}_{\text{eff}}$, which quantifies the relative velocity of cylindrical material layers, is

$$\dot{\gamma}_{\text{eff}}(r) = -r\frac{d\omega}{dr}, \tag{3}$$

where $\omega = \dot{\delta} = v_\theta / r$ is the local rotation velocity of the material (v_θ is the tangential velocity). The shear stress decrease from the inner to the outer tool induces a strain heterogeneity in the gap so that we must distinguish the apparent (or macroscopic) variables from the effective (or local) variables. In this context the data will first be considered in the standard form, i.e., in terms of the (imposed) *apparent shear stress*,

$$\tau = \frac{M}{2\pi h r_1^2}, \tag{4}$$

and the *apparent deformation* (γ) in time (t),

$$\gamma \approx \frac{\alpha(t) r_1}{(r_2 - r_1)}, \tag{5}$$

in which α is the angle of rotation of the inner tool, or the *apparent shear rate*,

$$\dot{\gamma} \approx \frac{\Omega r_1}{(r_2 - r_1)}, \tag{6}$$

in which $\Omega = \dot{\alpha}$ is the rotation velocity of the inner cylinder.

The experiments will provide directly an *apparent constitutive equation*, in the form of a relation between τ (deduced from the imposed torque) and γ and/or $\dot{\gamma}$ (deduced from the measured rotation angle), and we will seek the *effective constitutive equation* in simple shear in the form of a relation between τ_{eff} and $\dot{\gamma}_{\text{eff}}$. Although the stress heterogeneity may appear as a source of complication for interpreting data, we emphasize that it has the great advantage to provide a controlled heterogeneity. This contrasts with the cone and plate geometry, which supposedly yields a homogeneous distribution of the stress, but in which with pasty materials some slight perturbations can lead to strong shear localization in an uncontrolled way [Coussot *et al.* (2002c); Coussot (2005)].

Note that as long as the material behaves as a simple viscoelastic solid the strain heterogeneity in the Couette gap does not affect the results from a qualitative point of view. Indeed, it may be shown [Coussot (2005)] that in that case γ_{eff} is proportional to r^{-2} (like the shear stress). For example, in that case the integration of (2) using (5) provides the relation between the effective deformation along the inner $[\gamma_{\text{eff}}(r_1)]$ or the outer tool $[\gamma_{\text{eff}}(r_2)]$ and the apparent deformation: $\gamma = (x + x^2)\gamma_{\text{eff}}(r_1)/2 = (1 + 1/x)\gamma_{\text{eff}}(r_2)/2$, with $x = r_1/r_2$. As a consequence, in the solid regime we can reasonably consider the apparent deformation as some kind of average value of the effective deformation in the gap.

III. RESULTS AND ANALYSIS

A. General characteristics

Let us first examine the overall aspect of the $\gamma(t)$ curves for a given time t_w and different stress levels. The behavior of the three materials (see Fig. 1) is qualitatively similar: three regimes may be distinguished depending on the stress level. For stresses smaller than a critical value τ_0, in logarithmic scale the $\gamma(t)$ curves exhibit first a plateau followed by a decrease towards negative values (see Fig. 1). This regime likely corresponds to the end of the relaxation of internal stresses stored during the preshear. This statement is confirmed by the fact that τ_0 decreases with t_w, which means that this effect tends to disappear as the previous shear history is forgotten. Although the $\gamma(t)$ curves appear to be time-shifted by a factor approximately proportional to t_w, as already observed for microgel beads [Cloitre *et al.* (2000)], suggesting that some aging process takes place, it is likely that stress relaxation effects play a significant role. This means that the initial state of the material in terms of internal stresses can hardly be well defined, and in order to circumvent this problem in the following we will assume that for $\tau > \tau_0$ the material rapidly forgets its possible uncomplete stress relaxation during the creep tests so that this effect can be neglected.

For stresses larger than τ_0 and smaller than a critical value τ_c the deformation first rapidly increases, then tends to reach a plateau. Over longer times $\gamma(t)$ goes on slightly increasing but tends to saturate (see Fig. 1). This effect likely corresponds to the fact that the initial structure of the material does not break but only undergoes a finite deformation even after long times. We suggest that this saturation of the deformation is the hallmark of the *solid regime* of pasty materials. The origin of the residual "flow" over long times

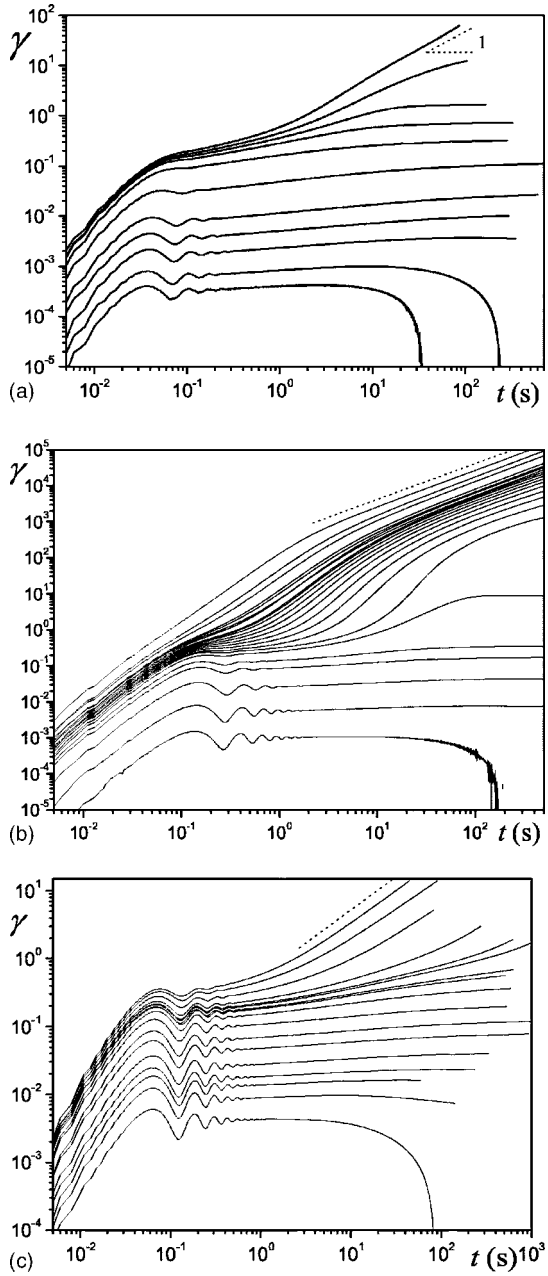

FIG. 1. Typical aspect of deformation vs time curves for different stress levels (τ) (from bottom to top) applied to our soft-jammed systems after a given time of rest: (a) Mustard (t_w=50 s) τ=0.4, 0.8, 2, 4, 8, 20, 40, 50, 54.8, 57.2, 60 Pa; (b) Bentonite suspension (t_w=60 s) τ=0.22, 1.1, 4.4, 11, 15.4, 22, 25.3, 28.6, 30.8, 33, 35.2, 37.4, 39.6, 41.8, 44, 48.4, 52.8, 59.4, 66, 110, 220 Pa; (c) Gel (t_w=20 s) τ=0.8, 4, 6, 8, 12, 20, 28, 40, 50, 56, 60, 63.2, 66.8, 70, 80, 90, 100 Pa. The inclined dotted line is the curve of slope 1.

in this (solid) regime will be discussed further below. In this context it seems possible to identify a critical deformation, γ_c, defined as the maximum deformation reachable in the solid regime. Note that, although in logarithmic scale the slope of the deformation vs time curve is never exactly zero, this does not correspond to a steady flow. Indeed, let us

assume that over some range of shear rates we have $\ln \gamma = \ln a + b \ln t$, in which $b \ll 1$, (in fact, in our data b continuously decreases with time). In that case $\dot{\gamma} = abt^{b-1}$, which decreases with t. This means that in this regime no stable flow, even extremely slow, can be expected over long times, in contrast with what was suggested for yield stress fluids [Barnes and Walters (1985); Barnes (1999)]. It is also worth noting that, for the mustard and the bentonite suspension, for τ very close to τ_c, the shape of the γ vs t curves is different: the deformation significantly increases in a first period, as if the material was evolving towards the liquid regime, then eventually saturates. This complex behavior is likely due to the fact that the material is initially not in its solid regime but evolves towards it as a result of further restructuring. In that case the critical deformation is more difficult to define.

For stresses larger than τ_c, over long times the $\gamma(t)$ curves tend to a straight line of slope 1 in logarithmic scale, which means that the deformation tends to increase at a constant rate, i.e., $\dot{\gamma}_{app} = \text{Cst}$. This corresponds to the *liquid regime* of the paste. Note that for the mustard and the bentonite suspension the transition between the solid and the liquid regime seems rather abrupt in terms of shear rate. Indeed, for a small increase in stress from below to beyond τ_c (see Fig. 1), the shear rate, found from the position of the line of slope 1 in the γ vs t curve, increases from zero in the solid regime to a finite value apparently larger than a critical, finite value ($\dot{\gamma}_c$). This corresponds to the viscosity bifurcation effect already observed for various pasty materials [Coussot *et al.* (2002a, b), Da Cruz *et al.* (2002)], but below we will further analyze these results and discuss how they may be affected by the heterogeneity in shear rate in the gap. For the gel there appears to be, between the range of steady flows and the range of flow stoppage, a range of stresses (say [63; 68 Pa]) for which it is not clear whether the material will ultimately stop or reach a steady flow over very long times. Since in such flows the sheared region is very thin (see below) this trend might be due to some particular evolutions of the structure of the gel along the solid surface. As a consequence, here we will assume that steady flows of the homogeneous gel can be obtained only beyond $\tau_c = 68$ Pa.

B. Solid regime

1. Flow start

In this regime, over short times (say less than 10 s) the deformation first rapidly increases then tends to reach a plateau but at the same time significantly oscillates (see Figs. 1 and 2). The reversibility of the deformation associated with this apparent plateau when the stress is released, which confirms the solid character of the material in this regime, will be demonstrated in the next paragraph. More precisely, we can expect that the material is basically viscoelastic in this regime. The trends observed over short times appear typical of a harmonic oscillator so that we can suggest that the oscillations correspond to the response of the viscoelastic material when it is suddenly submitted to a stress τ while there is significant inertia of the system (the inner cylinder and/or the material).

More precisely, let us assume that the material follows a simple viscoelastic model (Kelvin-Voigt model),

$$\tau_{eff} = G_0 \gamma_{eff} + \mu_0 \dot{\gamma}_{eff}, \tag{7}$$

in which G_0 and μ_0 are the elastic modulus and the viscosity of the material in the solid regime, respectively. In that case the solution of the momentum equation taking into account the rheometer inertia but neglecting the inertia of the material provides the following equation for the evolution of the apparent deformation:

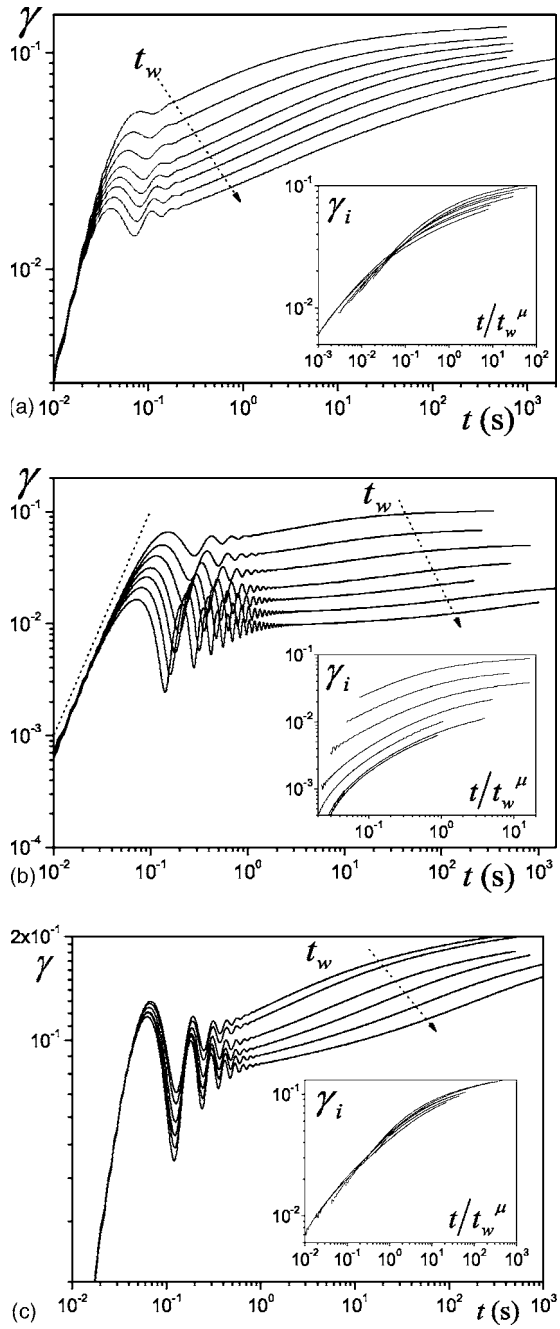

FIG. 2. Deformation as a function of the time for creep tests for different times of rest before shear (from top to bottom): (a) Mustard (τ=20 Pa) t_w=5, 10, 20, 50, 100, 200, 500 s; (b) Bentonite suspension (τ=4 Pa) t_w =20, 30, 50, 100, 200, 500, 1500 s; (c) Gel (τ=40 Pa), t_w=2, 5, 20, 60, 200, 600 s. Indicative dotted line of slope 2. The insets show the irreversible deformation (γ_i), estimated as the deformation minus the ratio of the applied stress to the initial elastic modulus $G(t_w)$, as a function of the time scaled by $t_w{}^{\mu}$.

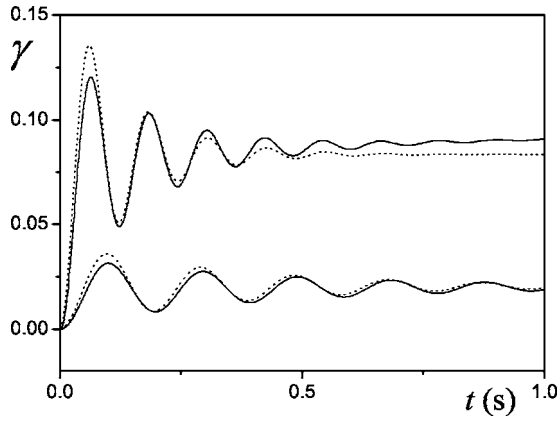

FIG. 3. Deformation in the very first time for creeps tests with gel (t_w=200 s) (upper curve) and with the bentonite suspension (t_w=100 s) (lower curve). The dotted curves correspond to the model (5) fitted to the experimental curves.

$$I\ddot{\gamma} + \mu\dot{\gamma} + G\gamma = \tau(t), \tag{8}$$

where I is the apparent inertia of the system, and $\mu=\varepsilon\mu_0$ and $G=\varepsilon G_0$, in which the value of ε takes its origin in our specific definition of the apparent deformation for such a wide-gap geometry: $\varepsilon=2/(x+x^2)$. Note that the value of I can be determined experimentally from a creep test without material since in that case the second and third terms of the left-hand side of (8) drop, leading to $\gamma=(\tau/I)t^2$.

When $4GI>\mu^2$ the solution of Eq. (8) for a stress step after some time at rest is

$$\gamma(t>0) = \frac{\tau}{G}\left[1 - \left(\frac{\sin(\omega t)}{\omega\theta} + \cos(\omega t)\right)\exp - \frac{t}{\theta}\right], \tag{9}$$

with $\theta=2I/\mu$ and $\omega=\sqrt{4GI-\mu^2}/2I$. According to (9) the initial deformation variations over very short times should be proportional to t^2, which is the case for our data (see Figs. 1 and 2), and the average level of the deformation γ_e of the (first) plateau is at first sight effectively proportional to τ (see below).

We can compare more precisely the predictions of this model with our data in the oscillation regime by fitting the values of θ and ω to the γ vs t curves in the initial range of times. It appears that for the gel and the bentonite suspension the agreement between theory and experiments is very good (see Fig. 3), especially for sufficiently large t_w and for stresses not too close to τ_c. For short times of rest (say less than 100 s for the bentonite suspension and 60 s for the gel) there is some slight discrepancy which increases as t_w decreases. This discrepancy also increases as the stress approaches τ_c. In fact, in those cases the frequency and amplitude decay of the oscillations are still well predicted by the model but the amplitude of the experimental asymptotic deformation (before the aging stage) is slightly larger than predicted by theory. This suggests that for short times of rest or when the stress approaches τ_c there is some significant, additional liquid or plastic flow during the very first times of flow which is not taken into account in the Kelvin-Voigt model. This effect may in particular be observed in Fig. 4, where we plotted the plateau deformation (γ_e) as a function of the stress: γ_e departs from a straight line as the stress approaches τ_c. In contrast the frequency of oscillations is independent of

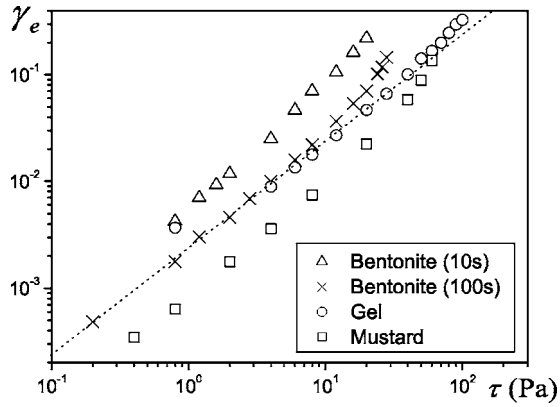

FIG. 4. Level of the apparent plateau of deformation after a short time of creep flow as a function of the stress level: Mustard (t_w=50 s); gel (t_w=20 s); bentonite (20 °C) (t_w=10 s and t_w=100 s). Indicative dotted line of slope 1.

the stress level (cf. Fig. 1). In the following the value of the elastic modulus as deduced from the frequency of oscillations will be referred to as the elastic modulus (G) in the solid regime.

For the mustard the things are slightly more complex: the oscillations rapidly damp but the average deformation goes on significantly increasing [see Fig. 2(a)]. This suggests that its behavior could be modeled by two Kelvin-Voigt components with different parameters in series. Indeed, for such a model one of the various possible aspects of the theoretical creep curve as a function of the relative values of parameters is analogous to our experimental creep curve with the mustard. In the following we will omit this complexity and assume that the mustard behavior approximately follows a simple viscoelastic model, and we will determine the elastic modulus from the frequency of the main oscillations.

2. Thixotropy

For thixotropic materials a standard procedure consists of estimating the evolution of the yield stress as a function of the time of rest. In that case the yield stress was generally found to increase as a power law of the time of rest [Alderman *et al.* (1991); Huynh *et al.* (2005)]. However, in practice the yield stress is often determined from a single increasing stress ramp during which the material can restructure before reaching the stress level associated with its effective initial yield stress. As a consequence the yield stress value significantly depends on the timing of the ramp. This effect seems to play a role also in creep tests (see above, in particular for the bentonite suspension and the mustard), so that the yield stress does not appear as a perfectly well-defined intrinsic property of the material. In this context, in order to precisely quantify thixotropy it seems more relevant to observe the evolutions of the elastic modulus with the time of rest. [In the specific case when the critical deformation finds a clear definition and does not vary with the time of rest and when the behavior of the material is simply viscoelastic in the solid regime, we can obtain a rough estimate of the yield stress evolution from $\tau_c = G\gamma_c$.]

Here, we observe (see Fig. 5) that G increases logarithmically with t_w,

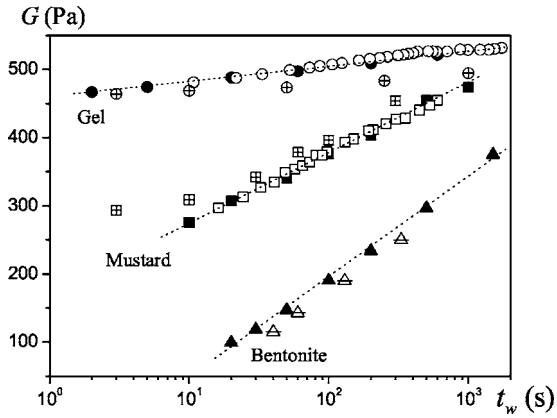

FIG. 5. Elastic modulus of the gel (squares), the mustard (circles), and the bentonite suspension (triangles), after different times of rest following preshear as deduced from the initial oscillations in creep curves (filled symbols), from dynamic tests (empty symbols), and from deformation recovery after stress release (crossed symbols). In order to gather all the data in the same figure, for the mustard the data presented here correspond to one-third the effective value of the elastic modulus. In recovery we have represented $G(t_w+t'_w)$ for the bentonite suspension and $G(t'_w)$ for the mustard and the gel.

$$G = \kappa \ln\left(\frac{t_w}{t_0}\right). \tag{10}$$

This result is similar to that obtained for the elastic modulus of silica suspensions [Derec *et al.* (2003)] as deduced from conventional dynamic tests. From dynamic tests we also determined the elastic modulus G' as a function of the time of rest after preshear. It appears that G' takes values almost exactly equal to those of G (see Fig. 5), which confirms the validity of our approach concerning the estimation of G, and suggests that these tests for characterizing the thixotropy of pasty materials in the solid regime are robust. It is worth noting that this procedure makes it possible to detect thixotropy in materials for which such effects were generally not detected so far (e.g., for the gel). Also note that for now we are unable to give a physical meaning to the parameter t_0 in (10).

3. Aging

Although when a stress is comprised between τ_0 and τ_c the deformation tends to saturate and the shear rate correspondingly decreases to zero, an effect which was considered as the hallmark of the solid regime, the residual increase of the deformation over long time remains to be explained. Note that although the effective deformation is not homogeneous in the gap (see Sec. II C) in the solid regime as defined above there is no liquid region and the evolution of the apparent deformation reflects some kind of average aging in the gap. This residual deformation increase might be explained by some additional, slow viscous flow, while the material would keep its solid behavior. In that case this deformation would be reversible, being recovered after stress release. In order to check this possibility we carried out tests consisting to release the stress after a certain time (t'_w) of creep (see Fig. 6). For small values of t'_w we observe that the deformation undergone at the time t'_w is subsequently entirely recovered after a sufficient time of relaxation. For larger t'_w there is an initial drop of γ followed by a slow decrease towards a residual value (γ_i) which increases with t'_w. Thus, in contrast with the behavior of a viscoelastic solid, the deformation is not fully recovered after stress release and the

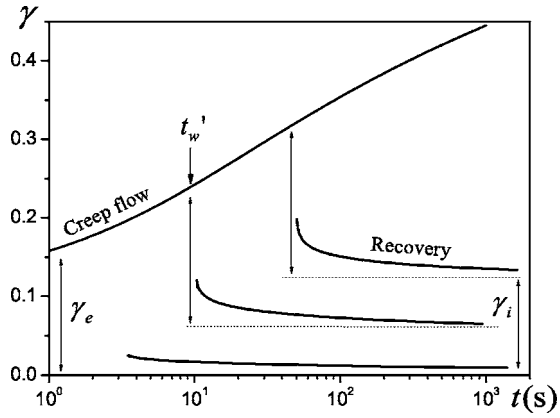

FIG. 6. Typical aspect of deformation recovery for stress release after different times (t'_w) of creep flow under a given stress (40 Pa) for a jammed system (here the gel). The level of the asymptotic elastic recovery is represented by dotted lines, from which we deduce the residual deformation γ_i.

residual, irreversible deformation (γ_i) increases with the time of flow (see Fig. 6). This effect was already observed for a model colloidal suspension [Petekidis *et al.* (2004)] and for a Carbopol suspension [Uhlherr *et al.* (2005)], and our results show its general character for pasty materials of various structures. This partial recovery nevertheless suggests that the material still behaves as a viscoelastic solid in this regime. This is confirmed by the fact that, during this recovery, the deformation exhibits oscillations in time analogous to those observed for a positive stress step (see above). Since the deformation for a Kelvin-Voigt model is described by an equation analogous to (9), we can again compute an apparent elastic modulus from the oscillation frequency.

Different evolutions of this elastic modulus in time are observed depending on the material (see Fig. 5). For the gel it remains constant, which means that during creep flow the material can no longer restructure as it could do during a rest period; for the bentonite suspension the evolution of this elastic modulus in the form $G(t_w+tw')$ is quite similar to those of G or G' at rest, which means that during creep flow the material goes on restructuring as if it were at rest; for the mustard the evolution of the elastic modulus in the form $G(t'_w)$ is similar to those of the elastic modulus at rest, so that all occurs as if the initial deformation during the stress step rejuvenated the material, which then starts again evolving as if it was at rest.

As already mentioned, the initial elastic contribution (at the plateau) may slightly differ from that expected using the elastic modulus (see Sec. III B 1). Moreover, a further analysis of our data according to the above considerations also showed that, except for the bentonite suspension during creep flow, this elastic contribution further slightly increases then rapidly tends to a constant value over longer times while γ_i goes on increasing. For the bentonite suspension the strong increase of the elastic modulus in time leads to an additional irreversible deformation. For all materials, from our recovery tests after different times t'_w during a creep flow, we observe that γ_i increases logarithmically with t'_w (see Fig. 7). Since the creep tests were carried out at arbitrary stress values in Fig. 7 we plotted $\gamma_i \tau_c / \tau$ as a function of t'_w, in order to test whether the irreversible deformation is somewhat proportional to the elastic deformation for the same stress. It is remarkable that for the mustard and the bentonite the curves are similar, which suggests some similarity of the aging process in yet very different materials.

These trends are reminiscent of the creep flow curves for glasses. In that case the

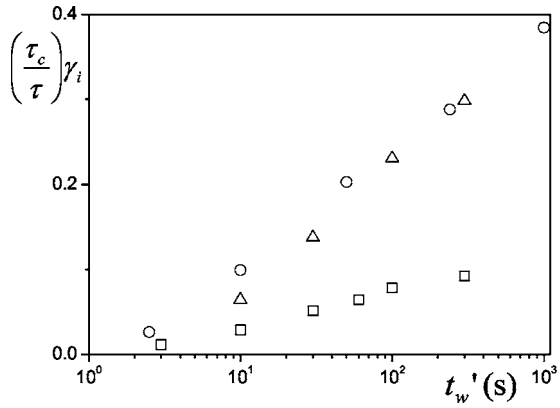

FIG. 7. Asymptotic residual deformation (scaled by the factor τ_c/τ) after stress release as a function of time of creep flow (shown in Fig. 2) for the gel (squares), the mustard (circles), and the bentonite suspension (triangles).

residual deformation was considered as taking its origin in an *aging process* [Struik (1978)], and the creep curves were shown to fall along a master curve when the deformation was plotted as a function of the time scaled by t_w^{μ}, where μ is a factor between 0.65 and 1. Also, for a model pasty material it was shown that this scaling was sufficient for obtaining a master curve [Cloitre *et al.* (2003)]. With our materials we also observe that the $\gamma(t)$ curves tend to have a similar shape shifted towards larger time as t_w increases. However, with our different pastes a simple scaling of the time with a power of t_w does not make it possible to get a single master curve. This is not unexpected since for our materials the initial plateau level also decreases with the time of rest. In order to follow solely the irreversible deformation, we suggest to withdraw from the actual deformation an estimation of the elastic contribution, i.e., $\tau/G(t_w)$, by using the predictions of the model (10) fitted to the data for $G(t_w)$ (we indeed did not carry out systematic recovery experiments for all t_w values providing straightforward values for γ_i). Under these conditions it appears that the creep curves as a function of t/t_w^{μ} (in which the value of μ is reported in Table I) fall rather well along a master curve (see the insets of Fig. 2) for sufficiently large t_w (note that a more precise estimation of the residual deformation in time, as it was done for a specific time of rest in Fig. 7, would likely yield similar straight lines for the different times of rest in semi-logarithmic scale).

TABLE I. Rheological parameters of the different materials in the liquid regime (τ_c, n, k) from creep tests presented in Fig. 1, and in the solid regime (κ, t_0, μ) from creep tests of Fig. 2.

Material	Gel	Bentonite	Mustard
τ_c (Pa)	68	23.1	55.7
n	0.28	0.625	0.333
k (Pa.s^n)	75.3	2.7	27.7
$\dot{\gamma}_c$ (s^{-1})	0.73	31	8.3
κ (Pa)	9.5	64	135
t_0 (s)	2.10^{-21}	4.6	0.022
μ	0.7	1	0.8

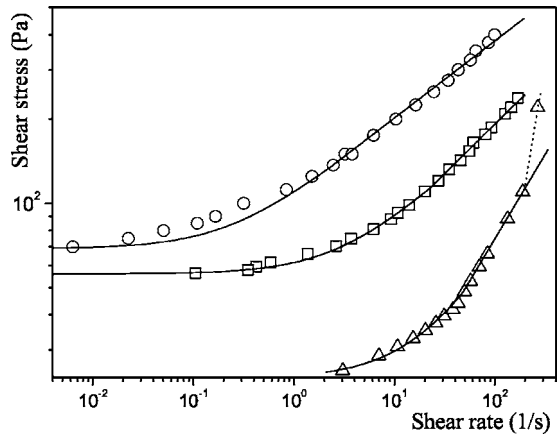

FIG. 8. Apparent flow curve (i.e., set of apparent shear stresses as a function of apparent shear rates) for the gel (circles), the mustard (squares), and the bentonite suspension (triangles). The continuous lines correspond to the constitutive equation (12) fitted to data.

C. Liquid regime

From the creep curves we can compute the apparent steady shear rate associated with each value of the apparent shear stress imposed beyond τ_c. The corresponding data provide the apparent flow curve of the material (see Fig. 8). The results are qualitatively similar for all materials: in agreement with usual observations for pasty materials [Coussot (2005)] the apparent flow curve is that of a simple yield stress fluid, which might be for example represented by a Herschel-Bulkley model (i.e., $\tau=\tau_c+\chi\dot{\gamma}^p$ for $\tau>\tau_c$, $\dot{\gamma}=0$ for $\tau<\tau_c$, in which χ and p are two material parameters). For the bentonite suspension beyond some critical shear rate value (about 200 s^{-1}) the flow curve seems to turn to another power-law model with a larger exponent, a regime which likely corresponds to some flow instability (Taylor-Couette flow instability or turbulence). The generalized Taylor number $[\rho\dot{\gamma}^2(r_2-r_1)^{5/2}(r_1+r_2/2)^{1/2}/\tau r_1$, in which ρ is the fluid density] [Coussot (2005)] for the first point associated with this regime is indeed equal to 44, that is just above the critical value (i.e., 42) for which the Taylor-Couette instability should occur. For the gel and the mustard it was not possible to clearly identify this regime because the material just started to flow out of the gap, which suggests that strong normal stress effects took place at that time.

A further analysis of these data, taking into account the heterogeneity of the shear stress distribution, shows that the effective behavior does not correspond to a simple yield stress behavior, i.e., with a shear rate tending to zero as the shear stress tends to the yield stress. Indeed, from the data of Fig. 1 we can deduce the value of the critical apparent stress τ_c (along the inner cylinder) below which the flow eventually stops. Since the shear stress within the gap continuously decreases from the inner to the outer cylinder, for an apparent stress τ slightly larger than τ_c, in steady state only the fluid layers situated sufficiently close to the inner cylinder will be sheared. More precisely, we readily find from Eqs. (1) and (4) that when $\tau<\tau_c(r_2/r_1)^2$ the material is sheared up to the critical distance $r_c=r_1\sqrt{\tau/\tau_c}$ so that the thickness of the sheared region is $e=r_1(\sqrt{\tau/\tau_c}-1)$. Now, taking into account the effectively sheared region, we can compute a more precise, though still apparent, shear rate,

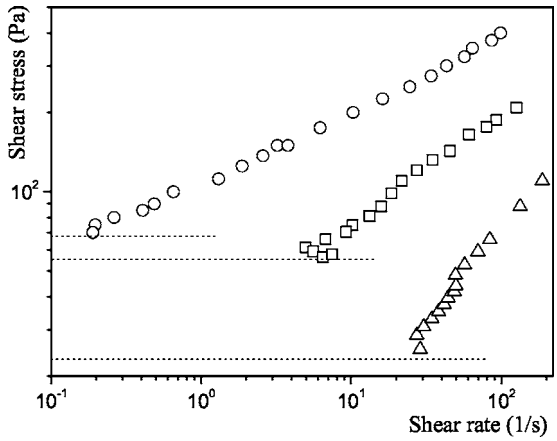

FIG. 9. Apparent flow curve taking into account the effectively sheared thickness within the gap (i.e., set of τ vs $\dot{\gamma}_{app}{}^*$) for the gel (circles), the mustard (squares), and the bentonite suspension (triangles). The horizontal dotted lines indicate the level of the yield stress of each material.

$$\dot{\gamma}_{app}{}^* = \frac{\Omega r_1}{e} \text{ for } \tau_c < \tau < \tau_c(r_2/r_1)^2 \text{ and } \dot{\gamma}_{app}{}^* = \dot{\gamma}_{app} \text{ for } \tau > \tau_c(r_2/r_1)^2. \quad (11)$$

Plotting τ vs $\dot{\gamma}_{app}{}^*$, we obtain a more precise apparent flow curve which, as long as the sheared layer can be considered as a continuum medium with properties similar to those of the complete sample, tends to the effective flow curve when $\tau \to \tau_c$ since then the shear stress can be considered as constant in the sheared layer and the shear rate is homogeneous.

In this representation (see Fig. 9) the flow curves of our pasty materials have a shape close to a straight line in logarithmic scale, which suggests a power-law behavior. The striking point is that for each material this line clearly intersects the horizontal axis associated with the yield stress level at a finite shear rate value. Thus, the minimum level of shear rate that can be reached in steady state differs from zero, in contrast with the predictions of conventional simple yield stress model (e.g., the Herschel-Bulkley or Casson models). For example, for a Herschel-Bulkley model it may be shown from the velocity profiles expressions [see Coussot (2005)] that $\dot{\gamma}_{app}{}^* \approx (M/2\pi h r_1{}^2 k)^{1/n}(n/n+1) \times (\sqrt{\tau/\tau_c}-1)^{1/n}$, which tends to zero when $\tau \to \tau_c$.

These observations are in agreement with direct observations of the velocity profiles of pasty materials within a Couette geometry. In that case it was shown that the minimum shear rate, i.e., along the liquid-solid interface in the sheared region, is generally nonvanishing [Coussot *et al.* (2002a); Da Cruz *et al.* (2002)]. For the bentonite suspension the value found by MRI for a slightly different solid fraction [Raynaud *et al.* (2002)], namely 24 s^{-1}, is quite consistent with ours (see Fig. 9). For the gel a smaller value (of the order of 0.04 s^{-1}) than ours (see Fig. 9) was found with another hair gel [Baudez *et al.* (2004)].

In this context it seems more realistic to represent the effective behavior of these pasty materials in steady state by a "truncated power-law" of the form

$$\tau_{eff} < \tau_c \Rightarrow \dot{\gamma} = 0; \quad \tau_{eff} > \tau_c \Rightarrow \tau_{eff} = k\dot{\gamma}_{eff}{}^n, \quad (12)$$

in which k and n are two material parameters which are in particular related to the yield stress and the critical shear rate via $k = \tau_c/\dot{\gamma}_c{}^n$. In Fig. 8 we also compared successfully the

apparent flow curve resulting from this effective behavior with our data (see the Appendix).

IV. PHYSICAL INTERPRETATION AND CONCLUSION

Although they may have very different structures, pasty materials exhibit qualitatively similar rheological properties. Indeed, a precise rheometrical study of these systems show that

(i) one can clearly distinguish a solid and a liquid regime, from the saturation of the deformation in time for the former and the steady increase of the deformation for the latter;
(ii) in the solid regime the material basically behaves as a viscoelastic solid and precise information concerning the elastic modulus may be obtained from the frequency of the oscillations in creep flows;
(iii) the thixotropy of the system at rest may be characterized more precisely from the elastic modulus than from the yield stress as a function of time;
(iv) in creep flow for a stress smaller than the yield stress the material undergoes residual irreversible deformations (called plastic deformation in the framework of mechanics of solid materials) which are reminiscent of aging in glasses;
(v) it may be demonstrated from conventional rheometrical tests that the solid-liquid transition is abrupt, namely in steady state the material cannot flow at an effective shear rate smaller than a critical value which differs from zero, in contrast with usual assumptions in this field;
(vi) the behavior of the material in the liquid regime is well represented by a truncated power-law model.

It is tempting to search some physical explanations to these common, specific characteristics, but since their structures differ this explanation must rely on some general, conceptual scheme, which goes beyond the specific structure of each material. In that aim we can first recall that aging and thixotropy in the solid regime may be associated with some similarities of material structures: the large (volume) concentration of elements in interaction forms a jammed structure in which the elements are embedded in potential wells due to the interactions with their neighbors; the great number of small (colloidal) elements in a liquid forms an out-of-equilibrium system which, as a result of the interactions and thermal agitation, progressively rearranges, i.e, at rest the elements fall in deeper potential. The latter effect leads to an increase of the apparent strength (elastic modulus or yield stress) of the system with the time of rest; in the solid regime the system can also progressively rearrange when it is submitted to a stress, which leads to further aging. Beyond a critical stress the structure breaks, which leads to the liquid regime. However, in steady flow the configuration goes on evolving: its is continuously broken due to flow but it keeps some tendency to restructure. Thus, following a previous suggestion [Coussot *et al.* (2002b)] the flow characteristics may be seen as the result of a competition between aging due to restructuration and rejuvenation due to flow. Depending on the flow rate either of these effects can become predominant, leading either to flow stoppage or flow at a constant shear rate but the balance of these effects defined a critical shear rate which is strictly positive. We also can assume that the tendency to restructuration in the liquid regime has something to do with the observed restructuration in the solid regime.

The above analysis suggests that there is some physical link between the properties in the liquid and the solid regime. Here, we attempt to roughly check the relevancy of this statement from a quantitative point of view on the basis of our data with materials with

very different microstructures. Let us assume that the structure state can be represented by some instantaneous elastic modulus of the material. In the solid regime this parameter has an obvious meaning; in the liquid regime it represents the elastic modulus that the material would have if it could be tested after an instantaneous stoppage in its actual structure. In this context, it is remarkable that the relative rate of restructuration of the material, i.e., dG/Gdt_w, taken arbitrarily at $t_w=10$ s, is proportional to $\dot{\gamma}_c$, which is proportional to the critical rate of destructuration in the liquid regime. Indeed, $dG/G\dot{\gamma}_c dt_w$ is equal to 0.0027 for the gel, 0.002 for the mustard, and 0.0034 for the bentonite suspension. This very approximate approach tends to confirm the probable link between aging properties at rest and the solid-liquid transition characteristics, and suggests that the abrupt transition between the solid and the liquid regime could result from some competition between retructuration and destructuration effects.

This very preliminary physical analysis of such data already suggests that there are interesting possibilities of understanding the physical origin and link of the solid and liquid behavior of pastes as soon as one can rely on a precise rheometrical characterization involving the effectively fundamental rheological parameters of the material, which was the basic objective of this study. For example, it will be interesting to look further and more systematically at the relationship between the corresponding rheological parameters for a given model material: the rate of restructuration at rest, the rate of increase of the irreversible deformation, the scaling parameter for the time in creep flows in the solid regime, the critical shear rate at the solid-liquid transition.

ACKNOWLEDGMENTS

The authors at Institut Navier work in the Laboratoire des Matériaux et des Structures du Génie Civil, joined laboratory (UMR113) of LCPC, ENPC, and CNRS. The authors acknowledge helpful comments of E. Weeks and C. Ancey on this work.

APPENDIX: APPARENT FLOW CURVE IN COUETTE FLOW FOR A FLUID FOLLOWING A TRUNCATED POWER-LAW MODEL

Using Eqs. (1)–(4) we can compute the apparent flow curve (in terms of τ vs $\dot{\gamma}$) of a material with a constitutive equation given by (12). We first integrate Eqs. (1), (3), and (12) to find the velocity along the inner cylinder [see also Coussot (2005)],

$$v_\theta(r_1) = \frac{n}{2}\dot{\gamma}_c\left[\left(\frac{r_c}{r_1}\right)^{2/n} - 1\right]r_1 \quad r_1 < r_c < r_2, \tag{A1}$$

$$v_\theta(r_1) = \frac{n}{2}\left(\frac{\tau}{k}\right)^{1/n}\left[1 - \left(\frac{r_1}{r_2}\right)^{2/n}\right]r_1 \quad r_2 < r_c. \tag{A2}$$

From (A1) and (A2) we can deduce the relations between the rotation velocity of the inner cylinder $[\Omega = r_1 v_\theta(r_1)]$ and the apparent shear stress in both cases. We thus deduce the apparent flow curve when the gap is partially sheared,

$$\tau = \tau_c\left[1 + K^*\frac{\dot{\gamma}}{\dot{\gamma}_c}\right]^n \quad \text{when } \tau_c < \tau < \tau_c(r_2/r_1)^2, \tag{A3}$$

in which $K^* = 2(r_2 - r_1)/nr_1$; and when the gap is fully sheared,

$$\tau = \left[\frac{2(r_2 - r_1)}{n r_1 (1 - (r_1/r_2)^{2/n})} \right]^n k \dot{\gamma}^n \quad \text{when } \tau > \tau_c (r_2/r_1)^2. \tag{A4}$$

Equations (A3) and (A4) provide the apparent flow curve of a material exhibiting a truncated power-law behavior, which appears to be similar to that for a Herschel-Bulkley behavior for shear stresses close to the yield stress [cf. (A3)] while it follows a power-law behavior with the same exponent as in the effective behavior for larger shear stresses.

In order to compare the predictions of this model with our data, we have used the value for the yield stress as determined from the creep tests, and fitted the values of $\dot{\gamma}_c$ and n on the apparent power-law behavior in the range $\tau > \tau_c (r_2/r_1)^2$ in the data of Fig. 8 (see the values in Table I). For the mustard and the bentonite suspension the agreement of this model with our data is very good (see Fig. 8) and the values obtained for $\dot{\gamma}_c$ are in excellent agreement with those observed by the further analysis of the apparent flow curve (see Fig. 9). For the gel there is a slight discrepancy (of the order of 10%) in the apparent flow curve predictions and a more significant discrepancy between the two critical shear rate values although their order of magnitude is similar. This is likely due to its specific behavior (see Sec. III A) when the sheared layer is small.

References

Alderman, N. J., G. H. Meeten, and J. D. Sherwood, "Vane rheometry of bentonite gels," J. Non-Newtonian Fluid Mech. **39**, 291–310 (1991).

Astarita, G., "Letter to the Editor: The engineering reality of the yield stress," J. Rheol. **34**, 275–277 (1990).

Barnes, H. A., "Thixotropy—A review," J. Non-Newtonian Fluid Mech. **70**, 1–33 (1997).

Barnes, H. A., "The yield stress—A review or "$\pi\alpha\nu\tau\alpha\ \rho\varepsilon\iota'$—Everything flows?," J. Non-Newtonian Fluid Mech. **81**, 133–178 (1999).

Barnes, H. A., and Q. D. Nguyen, "The use of the rotating vane geometry for non-Newtonian fluids—A review," J. Non-Newtonian Fluid Mech. **98**, 1–14 (2001).

Barnes, H. A., and K. Walters, "The yield stress myth?," Rheol. Acta **24**, 323–326 (1985).

Baudez, J. C., S. Rodts, X. Chateau, and P. Coussot, "A new technique for reconstructing instantaneous velocity profiles from viscometric tests—Application to pasty materials," J. Rheol. **48**, 69–82 (2004).

Bécu, L., P. Grondin, A. Colin, and S. Manneville, "How does a concentrated emulsion flow? Yielding, local rheology, and wall slip," Colloids Surf., A **263**, 146–152 (2004).

Bird, R. B., D. Gance, and B. J. Yarusso, "The rheology and flow of viscoplastic materials," Rev. Chem. Eng. **1**, 1–70 (1982).

Bonn, D., H. Tanaka, G. Wegdam, H. Kellay, and J. Meunier, "Aging of a colloidal 'Wigner' glass," Europhys. Lett. **45**, 52–57 (1999).

Britton, M. M., and P. T. Callaghan, "Two-phase shear band structures at uniform stress," Phys. Rev. Lett. **30**, 4930–4933 (1997).

Cappelaere, E., J. F. Berret, J. P. Decruppe, R. Cressely, and P. Lindner, "Rheology, birefringence, and small-angle neutron scattering in a charged micellar system: Evidence of a shear-induced phase transition," Phys. Rev. E **56**, 1869–1878 (1997).

Carnali, J. O., and M. S. Naser, "The use of dilute solution viscometry to characterize the network properties of Carbopol microgels," Colloid Polym. Sci. **270**, 183–193 (1992).

Chan Man Fong, C. F., G. Turcotte, and D. De Kee, "Modelling steady and transient rheological properties," J. Food. Eng. **27**, 63–70 (1996).

Cheng, D.C.-H., "Characterisation of thixotropy revisited," Rheol. Acta **42**, 372–382 (2003).

Cipelletti, L., S. Manley, R. C. Ball, and D. A. Weitz, "Universal aging features in the restructuring of fractal colloidal gels," Phys. Rev. Lett. **84**, 2275–2278 (2000).

Cloitre, M., R. Borrega, and L. Leibler, "Rheological aging and rejuvenation in microgel pastes," Phys. Rev. Lett. **85**, 4819–4822 (2000).

Cloitre, M., R. Borrega, F. Monti, and L. Leibler, "Glassy dynamics and flow properties of soft colloidal pastes," Phys. Rev. Lett. **90**, 068303 (2003).

Coleman, B. D., H. Markowitz, and W. Noll, *Viscometric flows of non-Newtonian Fluids* (Springer Verlag, Berlin, 1966).

Coussot, P., *Rheometry of Pastes, Suspensions and Granular Materials—Application in Industry and Environment* (Wiley, New York, 2005).

Coussot, P., A. I. Leonov, and J. M. Piau, "Rheology of concentrated dispersed systems in a low molecular weight matrix," J. Non-Newtonian Fluid Mech. **46**, 179–217 (1993).

Coussot, P., Nguyen, Q. D., Huynh, H. T., and Bonn, D., "Viscosity bifurcation in thixotropic, yielding fluids," J. Rheol. **46**, 573–589 (2002a).

Coussot, P., Nguyen, Q. D., Huynh, H. T., and Bonn, D., "Avalanche behavior in yield stress fluids," Phys. Rev. Lett. **88**, 175501 (2002b).

Coussot, P., Raynaud, J. S., Bertrand, F., Moucheront, P., Guilbaud, J. P., Huynh, H. T., Jarny, S., and Lesueur, D., "Coexistence of liquid and solid phases in flowing soft-glassy materials," Phys. Rev. Lett. **88**, 218301 (2002c).

Da Cruz, F., F. Chevoir, D. Bonn, and P. Coussot, "Viscosity bifurcation in foams, emulsions and granular systems," Phys. Rev. E **66**, 051305 (2002).

Decruppe, J. P., S. Lerouge, and J. F. Berret, "Insight in shear banding under transient flow," Phys. Rev. E **63**, 022501 (2001).

Derec, C., A. Ajdari, G. Ducouret, and F. Lequeux, "Rheological characterization of aging in a concentrated colloidal suspension," C. R. Acad. Sci., Ser IV: Phys., Astrophys. **1**, 1115–1119 (2000).

Derec, C., G. Ducouret, A. Ajdari, and F. Lequeux, "Aging and nonlinear rheology in suspensions of PEO-protected silica particles," Phys. Rev. E **67**, 061403 (2003).

Dullaert, K., and J. Mewis, "Thixotropy: Build-up and breakdown curves during flow," J. Rheol. **49**, 1213–1230 (2005).

Fielding, S. M., P. Sollich, and M. E. Cates, "Aging and rheology in soft materials," J. Rheol. **44**, 323–369 (2000).

Gopalakrishnan, V., S. A. Shah, and C. F. Zukoski, "Cage melting and viscosity reduction in dense equilibrium suspensions," J. Rheol. **49**, 383–400 (2004).

Hartnett, J. P., and R. Y. Z. Hu, "The yield stress—An engineering reality," J. Rheol. **33**, 671–679 (1989).

Hébraud, P., and F. Lequeux, "Mode-coupling theory for the pasty rheology of soft glassy materials," Phys. Rev. Lett. **81**, 2934–2937 (1998).

Herzhaft, B., L. Rousseau, L. Néau, M. Moan, and F. Bossard, "Influence of temperature and clays/emulsion microstructure on oil-based mud low shear rate rheology," SPEJ **8**, 211–221 (2003).

Hu, Y. T., and A. Lips, "Kinetics and mechanism of shear banding in an entangled micellar solution," J. Rheol. **49**, 1001–1027 (2005).

Huynh, H. T., N. Roussel, and P. Coussot, "Aging and free surface flow of a thixotropic fluid," Phys. Fluids **17**, 033101 (2005).

Liu, A. J., and S. R. Nagel, "Jamming is not just cool any more," Nature (London) **396**, 21–22 (1998).

Mas, R., and A. Magnin, "Rheology of colloidal suspensions: Case of lubricating greases," J. Rheol. **38**, 889–908 (1994).

Mewis, J., "Thixotropy—A general review," J. Non-Newtonian Fluid Mech. **6**, 1–20 (1979).

Mujumdar, A., A. Beris, and A. Metzner, "Transient phenomena in thixotropic systems," J. Non-Newtonian Fluid Mech. **2072**, 1–22 (2001).

Petekidis, G., D. Vlassopoulos, and P. N. Pusey, "Yielding and flow of sheared colloidal glasses," J. Phys.: Condens. Matter **16**, S3955–S3963 (2004).

Pignon, F., A. Magnin, and J. M. Piau, "Thixotropic colloidal suspensions and flow curves with minimum: Identification of flow regimes and rheometric consequences," J. Rheol. **40**, 573–587 (1996).

Ramos, L., and L. Cipelletti, "Intrinsic aging and effective viscosity in the slow dynamics of a soft glass with tunable elasticity," Phys. Rev. Lett. **94**, 158301 (2005).

Raynaud, J. S., P. Moucheront, J. C. Baudez, F. Bertrand, J. P. Guilbaud, and P. Coussot, "Direct determination by NMR of the thixotropic and yielding behavior of suspensions," J. Rheol. **46**, 709–921 (2002).

Rodts, S., J. C. Baudez, and P. Coussot, "From discrete to continuum flow in foams," Europhys. Lett. **69**, 636–642 (2005).

Roussel, N., R. Le Roy, and P. Coussot, "Thixotropy modelling at local and macroscopic scales," J. Non-Newtonian Fluid Mech. **117**, 85–95 (2004).

Roy, G., M. Pelletier, F. Thomas, C. Despas, and J. Bessieres, "Aggregation in Na-, K-, amd Ca—montmorillonite dispersions, characterized by impedance spectroscopy," Clay Miner. **35**, 335–343 (2000).

Salmon, J. B., A. Colin, S. Manneville, and F. Molino, "Velocity profiles in shear-banding wormlike micelles," Phys. Rev. Lett. **90**, 228303 (2003).

Seth, J. R., M. Cloitre, and R. T. Bonnecaze, "Elastic properties of soft particle pastes," J. Rheol. **50**, 353–376 (2006).

Shah, S. A., Y. L. Chen, K. S. Schweizer, and C. F. Zukoski, "Viscoelasticity and rheology of depletion flocculated gels and fluids," J. Chem. Phys. **119**, 8747–8760 (2003).

Sollich, P., F. Lequeux, P. Hébraud, and M. E. Cates, "Rheology of soft glassy materials," Phys. Rev. Lett. **78**, 2020–2023 (1997).

Spaans, R. D., and M. C. Williams, "Letter to the Editor: At last, a true liquid-phase yield stress," J. Rheol. **39**, 241–246 (1995).

Struik, L. C. E., *Physical Aging in Amorphous Polymers and Other Materials* (Elsevier, Houston, 1978).

Uhlherr, P. H. T., J. Guo, C. Tiu, X. M. Zhang, J. Z. Q. Zhou, and T. N. Fang, "The shear-induced solid-liquid transition in yield stress materials with chemically different structures," J. Non-Newtonian Fluid Mech. **125**, 101–119 (2005).

Usui, H., "A thixotropy model for coal-water mixtures," J. Non-Newtonian Fluid Mech. **60**, 259–275 (1995).

Varadan, P., and M. J. Solomon, "Direct visualization of flow-induced microstructure in dense colloidal gels by confocal laser scanning microscopy," J. Rheol. **47**, 943–968 (2003).

Viasnoff, V., and F. Lequeux, "Rejuvenation and overaging in a colloidal glass under shear," Phys. Rev. Lett. **89**, 065701 (2002).